Journal of Applied Polymer Science

WILEY

Applied Polymer SCIENCE

RESEARCH ARTICLE

Fabrication and Comparative Evaluation of Psyllium Husk Polysaccharide-Based Lyophilized, Electrospun and Three-Dimensional Printed Scaffolds for Functional Performance of Primary Hepatocytes

Sushmitha Paulraj | Dhanvi Vedantham | Pooja Kumari | Priya Singh | Snehlata Yadav | Sanjeev Kumar Mahto

Tissue Engineering and Biomicrofluidics Laboratory, School of Biomedical Engineering, Indian Institute of Technology (Banaras Hindu University), Varanasi, Uttar Pradesh, India

Correspondence: Sanjeev Kumar Mahto (skmahto.bme@iitbhu.ac.in)

Received: 6 November 2024 | **Revised:** 13 March 2025 | **Accepted:** 13 March 2025

Funding: This work was supported by Science and Engineering Research Board, CRG/2020/000235.

Keywords: 3D printing | electrospinning | hydrogel | lyophilization | psyllium husk polysaccharide | tissue engineering

ABSTRACT

Psyllium husk is known for its therapeutic value and is abundantly used in food, medicinal, and nutraceutical applications. In the present study, we have explored the potential of psyllium husk polysaccharide hydrogel either alone or in combination with gelatin for the culture and maintenance of adult rat hepatocytes. We have designed and fabricated electrospun nanofibrous sheets, three-dimensional (3D) printed, and lyophilized scaffolds using psyllium husk polysaccharide. Primary hepatocytes were harvested from the rat liver by the double perfusion method using collagenase. Results showed that all the scaffolds exhibited porous space in a similar size range of 100 to 250 μm, with 3D printed and lyophilized scaffolds within the range of 200–240 μm and 60–190 μm, respectively, which is reported to support the culture and performance of hepatocytes. Furthermore, morphology and viability characterization using MTT assay revealed that all the scaffolds displayed a remarkable viability of primary hepatocytes (~280%) and a significant level of aggregate formation compared to those on collagen-coated 2D substrates. All the 3D scaffolds supported hepatocyte secretion of albumin (0.1–0.6 mg/mL) and urea (20 to 180 μg/mL) into the extracellular fluid. Although all the scaffolds exhibited enhanced spheroid formation, viability, and metabolic functions, 3D printed (75-3DP) and electrospun (50-ES and 75-ES) scaffolds showed remarkable functional performances (albumin: 0.2–0.6 mg/mL; urea: 40–180 μg/mL) comparatively.

1 | Introduction

The liver, being an important organ for detoxification, metabolism, and homeostasis, is prone to several pathological conditions due to metabolic stress, infections, and diseases such as cirrhosis, hepatocellular carcinoma, or autoimmune disorders [1]. Severe hepatic injury compromises the regenerative efficiency of the liver, making liver transplantation the sole available treatment. However, a shortage of appropriate donors and immune rejection are major hurdles to prompt treatment [2]. To address this issue, the generation of biologically mimetic and functional bio-scaffolds, as a part of tissue engineering, has shown great promise in the development of three-dimensional in vitro hepatic tissue models to enable accurate replication of the tissue's microenvironment for supporting liver regeneration [3]. For liver tissue engineering (LTE) approaches, primary hepatocytes are considered a physiologically equivalent in vitro model for understanding liver-specific functions, drug metabolism, and hepatotoxicity [4].

A suitable substrate for culturing is highly desirable to retain the hepatocyte's specific morphology and aggregate (spheroid) formation, similar to sinusoid formation in vivo [5]. Furthermore, three-dimensional culture is preferred for restricted cell spreading and enhanced cellular polarity [6]. One of the key challenges in guiding the cell's behavioral and clinical outcomes lies in replicating its microenvironment and microarchitecture, called the extracellular matrix (ECM), which governs the phenotype and fate of living cells [7]. Several biomaterials have been developed through various approaches for fabricating scaffolds that mimic the ECM of the liver cell in particular. Some natural hydrogels used for LTE include hyaluronan [8], alginate [9], polyhydroxyalkanoates [10], agarose [11], cellulose [12], and collagen [13, 14]. Most of these are a part of ECM and hence show good growth response and excellent biocompatibility; however, they exhibit low mechanical strength, batch-to-batch variability, and ethical concerns for clinical uses [15]. Modifications of these natural biomaterials to produce synthetic or semi-synthetic hydrogels are known to increase the mechanical stability and to reduce the immunogenicity, while compromising bioactivity and viscoelasticity [16]. Such synthetic biomaterials include poly(ethylene glycol) [17], polyisocyanopeptide [18], and poly(lactide-co-glycolide) acid [19]. Researchers have attempted to address the limitations of mechanical stability and cell affinity of the fabricated scaffolds by incorporating materials such as nanofibrils [20], nanocurcumin [21], reduced graphene oxide [22], and cellulose acetate nanofibers [23]. The complex liver structure impedes its reproducibility using 3D scaffolds, a reason why liver-supporting scaffolds are not progressing to the clinical phase. Recently, several modifications and advancements were exerted to develop liver-specific scaffolds. Chitosan was modified to enhance the adhesion of hepatocytes through receptor-ligand interaction (ASGPR-galactose interaction) [24, 25]. In addition, hexagonal design [26] and interconnected porous architecture [27] of 3D scaffolds were also found to enhance hepatocyte functioning. Although significant progress has been made in developing appropriate scaffolds for liver tissue engineering, some key challenges still need to be addressed. They include a suitable scaffold material, fabrication technology, incorporation of moieties to enhance cellular functioning, and improved spatial design of the 3D scaffolds [28], and so forth.

A commonly used method for the fabrication of 3D scaffolds is freeze-drying, also known as lyophilization, which yields an acceptable range of interconnectivity between the pores [29]. Nevertheless, control over the pore size remains a concern in such lyophilized scaffolds [30]. Another emerging technology for low-cost, robust scaffold fabrication is electrospinning. The polymer solution is extruded from a hypodermic needle by a high-voltage power supply to generate fibrous forms of size range micro/nano-meter, similar to the native extracellular matrix (ECM) to facilitate cell/tissue function at the physiological level. It applies the principle that upon high-voltage, an electrostatic field is generated on the extruding droplet, which in turn creates the repulsive force between the charged particles, thereby overcoming the surface tension of the solution and formation of a jet of fibers on the collector [31]. Similarly, 3D printing is an enabling technology that supports the fabrication of physiologically comparable 3D scaffolds with similar architecture and greater intricacy through the layer-by-layer deposition of biomaterials [32]. It is therefore considered very promising for applications in scaffold development, biofabrication, and regenerative medicine.

In this work, we have evaluated the potential of psyllium husk polysaccharide hydrogel, either alone or in combination with gelatin, for the culture and maintenance of primary adult rat hepatocytes. *Plantago ovata*, also referred to as isabgol or psyllium husk, is a plant-based polysaccharide mainly consisting of hemicellulose, which is made up of a xylan framework connected with arabinose, rhamnose, galactouronic acid, galactose, and glucose [33, 34]. We have designed and fabricated lyophilized scaffolds, electrospun nanofibrous sheets, and 3D-printed scaffolds using psyllium husk polysaccharide. Primary hepatocytes were cultured on all the fabricated 3D scaffolds. Morphological characterization, such as aggregate formation was observed using microscopy techniques to assess the potential of all the scaffolds. In addition, the viability assay and metabolic functioning of hepatocytes, such as albumin and urea secretion were estimated after culturing primary hepatocytes on the prepared 3D scaffolds. Appropriate formulation consisting of psyllium polysaccharide-based hydrogel either alone or accompanied with gelatin was optimized to develop rheologically spinnable and printable solutions for fabricating lyophilized scaffolds, electrospun nanofibrous sheets and 3D printed scaffolds. The scaffolds were further chemically cross-linked by EDC-NHS to enhance their mechanical strength and stability in the physiologically comparable medium.

2 | Materials and Methods

Psyllium husk powder (Satnam Psyllium Industries, Gujarat, pale-buff colored, 99% purity with particle size ~150 μm), Gelatin (HiMedia, TC041-500G), *N*-(3-Dimethylaminopropyl)-*N′*-ethylcarbodiimide hydrochloride (EDC) (HiMedia, RM1817-25G), *N*-hydroxysuccinimide (NHS), 99% (Sigma-Aldrich, 130672-25G), phosphate-buffered saline (PBS), distilled water and absolute ethanol 99.9% of high analytical grade, 10 mL syringe with Luer-Lok Tip (BD, Ref-303064), 22G metallic blunt-end needle, polyvinyl alcohol (PVA) (HiMedia, GRM6171-500G), Dulbecco's modified eagle medium (DMEM) high glucose (HiMedia, AL007A-500ML), fetal bovine serum (FBS) (RM9955-500ML), Antibiotics—10,000 U penicillin and 10 mg streptomycin (HiMedia, A001A-500ML), Hank's balanced salt solution (HBSS) (HiMedia, TL1010-500ML), collagenase type IV (Merck, C4-28-100MG), collagen I rat tail (Gibco, A10483-01), bovine serum albumin (BSA) (HiMedia MB083-25G), Insulin (HiMedia, TCL125-10ML), hydrocortisone (Sulab, Product no. 4166), were used in the following experiments.

2.1 | Fabrication of Psyllium Husk Polysaccharide-Based Scaffolds

Psyllium husk (PH) powder and gelatin (G) powder were mixed in a suitable solvent in different ratios, and molded into scaffold materials using techniques such as 3D printing, electrospinning, and lyophilization (Table 1). For making (i) 3D printed scaffolds, the blended ink mixtures were incubated at 30°C for 12 h prior to printing; (ii) for electrospun fibrous scaffolds, the spinning solution was freshly prepared in polyvinyl alcohol (PVA) solvent and was subjected to electrospinning; and (iii) for the lyophilized scaffolds, the solution after preparation was stored at −80°C until freeze-drying. The parameters for scaffold

fabrication using individual techniques are depicted in Figure 1. All the scaffolds after their fabrication were crosslinked using EDC-NHS (25–12.5 mM) in 90% ethanol solvent for 24 h. The scaffolds were then rinsed thoroughly using distilled water before being used for further experiments. The lyophilized scaffolds were again freeze-dried after crosslinking and washing.

2.2 | Morphological Characterization of Fabricated 3D Scaffolds

The morphological analysis of all the scaffolds was assessed through scanning electron microscopy (SEM) images using Nova nanoSEM 450 and Jeol benchtop SEM (JCM-6000PLUS). The 3D-printed scaffolds were lyophilized to obtain a dry scaffold for SEM imaging.

2.3 | ATR-FTIR Spectroscopy of the Fabricated 3D Scaffolds

All the fabricated scaffolds were analyzed for infrared spectra (Alpha Bruker Eco-ATR with ZnSe attenuated total reflection accessory) under resolution 4 cm^{-1} with 36 scans for the range 500–4000 cm^{-1}, to understand the spectra of crosslinked scaffolds.

2.4 | Swelling and Degradation Studies

All the fabricated 3D scaffolds were dried completely, and their dry weight was taken as the initial weight (W_0). The scaffolds were then immersed in the PBS (pH 7.4) solution and kept at 37°C. From this point, the scaffolds were weighed periodically

TABLE 1 | Scaffold fabrication methods and composition of blended formulations used.

Scaffold fabrication method	Sample code	Psyllium husk (g)	Gelatin (g)	Solvent	Solvent volume (mL)
3D printing	75-3DP	0.6	0.2	Water	10
	100-3DP	0.8	—	Water	10
Electrospinning	50-ES	0.2	0.2	6% PVA	14
	75-ES	0.3	0.1	6% PVA	14
	100-ES	0.4	—	6% PVA	14
Lyophilization	50-L	0.4	0.4	Water	10
	75-L	0.6	0.2	Water	10
	100-L	0.8	—	Water	10

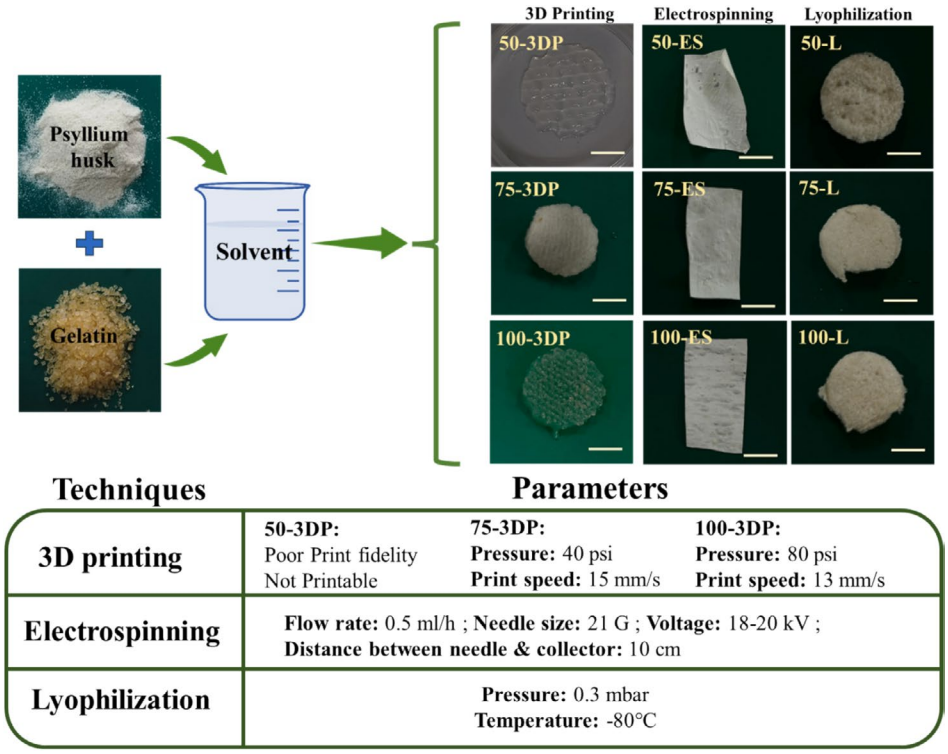

FIGURE 1 | Different techniques and their optimized parameters for fabricating psyllium polysaccharide-based 3D scaffold. [Color figure can be viewed at wileyonlinelibrary.com]

(for 3 days) to get their wet weight (W_t). The degree of swelling of the scaffolds was calculated using the following formula,

$$\text{Degree of swelling}\,(\%) = \frac{(W_t - W_0)}{W_0} \times 100$$

Microscopic investigation (SEM analysis) of the scaffolds immersed in PBS for 7 days was obtained to depict their degradation profile. The scaffolds were dried before microscopic investigation.

2.5 | Harvesting of Primary Hepatocytes From Rat Liver

The hepatocytes were isolated from Wistar rats by a two-step perfusion method [35]. The animals used in this study were approved by the Institute Animal Ethical Committee, Indian Institute of Technology (Banaras Hindu University). Briefly, the Wistar rat (150–200 g) was anesthetized by ketamine-xylazine injection (100/80 mg per 100 g of body weight) and an incision was made in its abdominal region using sterile surgical instruments. The liver was then resurrected, followed by performing in vitro perfusion in a sterile hood. A 24 G needle was used to perfuse calcium-free HBSS containing ethylenediamine tetraacetic acid (EDTA, 0.5 mM) to loosen the cell–cell junctions by depleting calcium ions, followed by perfusion with collagenase type IV enzyme buffer (0.05%) to digest the organ. The perfusion was performed through the portal vein of the liver. The organ was then disrupted mechanically to release cells, which were then washed with HBSS buffer repeatedly using centrifugation (50 rcf) to remove non-parenchymal cells. The isolated hepatocytes were cultured in DMEM, supplemented with 10% FBS and antibiotics, on collagen-coated plates. After 4 h, the medium was replaced by hepatocyte culture medium (DMEM high glucose, 0.02 mg/L epidermal growth factor (Cat.No. Z00333-50, GenScript), 7.5 mg/L hydrocortisone, 500 U/L insulin, 0.5% BSA) for the rest of the culture period.

2.6 | Culturing of Primary Hepatocytes on Prepared 3D Scaffolds

The UV-sterilized scaffolds were used in the following experiment. After isolating the hepatocytes, 1×10^6 cells were cultured on the scaffolds using DMEM high glucose supplemented with 10% FBS and antibiotics. After 4 h, cell-seeded scaffolds were rinsed with HBSS buffer and transferred to a new well plate to remove non-adhered cells, thereby replacing the culture medium with hepatocyte culture medium.

2.7 | Characterization of Primary Hepatocytes Isolated From Rat Liver

The hepatocytes isolated from rat liver were analyzed morphologically using a bright-field microscope (Nikon Ti-U, Japan). Fluorescent images of the hepatocytes cultured on collagen-coated plates were captured. The cells were fixed using 4% paraformaldehyde followed by treatment with 0.5% Triton X 100. 1% BSA was added as a blocking agent. The cells were then incubated with rhodamine-phalloidin conjugate (1X) and DAPI (1 μg/mL), after which they were rinsed thoroughly with PBS for observing the fluorescent stained cells. Similarly, for glycogen staining, cells were fixed with 4% paraformaldehyde, followed by 0.5% periodic acid and Schiff's reagent. The cells were then washed with PBS and observed under a microscope. For the albumin and urea assays, the hepatocyte-conditioned medium was used post-removal of dead cells by centrifugation. The concentration of albumin and urea secreted by the cells was assessed using a BCG method (AGD CliniPak, AGD-AL100) and a Berthelot method (Coral clinical systems), respectively. The protocol was followed according to the instructions provided by the kit. The standard graph was obtained for albumin and urea, based on which the concentration of albumin and urea secreted by hepatocytes seeded on the scaffolds was calculated.

3 | Statistical Analysis

Statistical analysis was performed using Origin software (OriginPro 2017). All the experiments were repeated in triplicates ($n = 3$) and represented as mean ± standard deviation. One-way ANOVA with Tukey's post hoc means of comparison was performed between the groups and is considered statistically significant when $p < 0.05$ (*), $p < 0.01$ (**), $p < 0.001$ (***).

4 | Results

4.1 | Morphology of the Fabricated Psyllium Polysaccharide-Based 3D Scaffolds

The morphology of the psyllium polysaccharide-based 3D scaffolds fabricated by 3D printing, electrospinning, and lyophilization techniques was studied using a scanning electron microscope (Figure 2). The image showed the different morphologies of the scaffolds fabricated using different techniques. The 3D-printed scaffolds were designed and fabricated to constitute both micro/meso pores and macropores. The 3D design, as exhibited in Figure 3, consists of a complex design with a well interconnected porous structure, which yielded a pore size of 200–240 μm when printed with a 22 G needle. When the printed construct was lyophilized, some micro/meso pores were observed to be formed on the printed strands, which might perform as a suitable anchoring site for the seeded hepatocytes. Whereas, the macropores in the printed scaffolds would help in uniform media and gas exchange throughout the scaffold, as well as uniform hepatocyte distribution throughout the scaffold during the time of seeding. In the electrospun scaffolds, the strands were deposited randomly, giving rise to nanofibrous morphology. It was also observed that the fiber thickness increased with an increase in psyllium husk content, with an average fiber thickness of 141.115 ± 4.58 nm (50-ES), 228.24 ± 7.82 nm (75-ES), and 253.45 ± 9.402 nm (100-ES). Nanofibers produced were observed free from bead formation, indicating a uniform distribution of the fibrous jet and the homogeneity of the prepared spinning solutions. The lyophilized scaffolds significantly exhibited roughness and irregularities in their appearance. They displayed uniformly

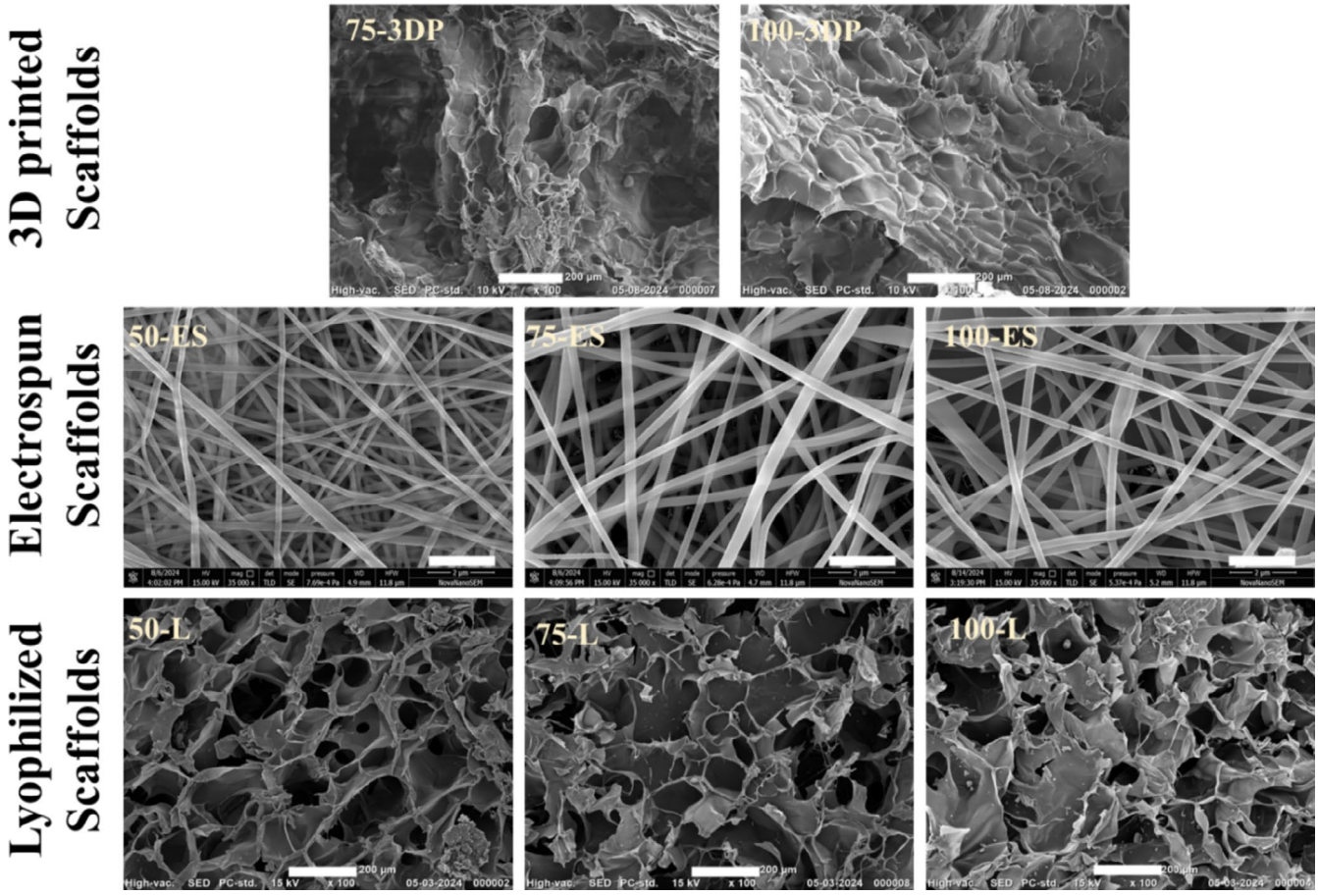

FIGURE 2 | Scanning electron microscopic images of 3D printed (scale bar: 200 μm), electrospun (scale bar: 2 μm) and lyophilized (scale bar: 200 μm) scaffolds depicting the morphological characteristics of the 3D scaffolds. [Color figure can be viewed at wileyonlinelibrary.com]

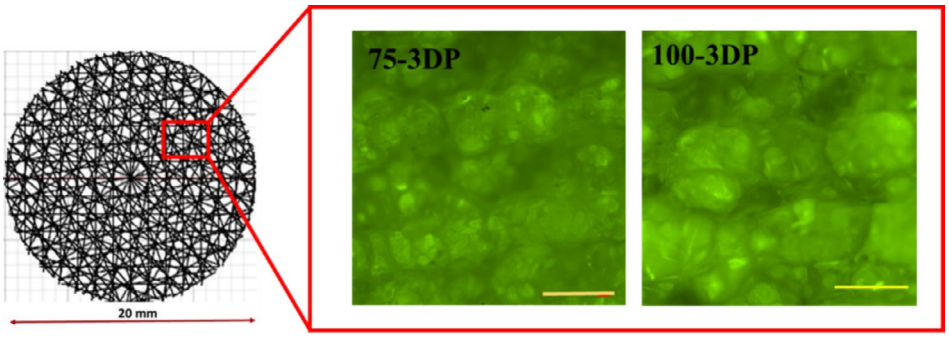

FIGURE 3 | 3D design and digital image of 3D printed scaffolds depicting the interconnected porous structure. Scale bar: 600 μm. [Color figure can be viewed at wileyonlinelibrary.com]

distributed, tightly packed interconnected pores with polyhedral shapes within the polymeric framework. The pore size of all the lyophilized scaffolds, that is, 100-L, 75-L, and 50-L was observed to be mostly in the range of 60–190 μm, suggesting the potential of the scaffolds for sustained cell growth and proliferation in a 3D environment.

4.2 | ATR-FTIR Spectroscopy

The ATR-FTIR spectrum shows the functional groups in the fabricated 3D scaffolds. In Figure 4, the spectrum of all the scaffolds shows a broad peak around 3300 cm^{-1} for characteristic —OH stretching. The narrow peak in the pure gelatin depicts the amide A group in the same region. Peaks at 2926 and 2877 cm^{-1} were observed for CH symmetric/asymmetric stretching (alkanes) in all the scaffolds. A peak around 1638 cm^{-1} for characteristic C═O was observed in all the samples, indicating the presence of the carboxylic acid —COOH group. A peak around 1544 cm^{-1} for amide II (N—H bending) and C—N stretching was present in all the scaffolds (except 100-3DP, 100-ES, and 100-L). A peak around 1033 cm^{-1} was observed for C—O stretching in all the prepared scaffolds, indicating the occurrence of an esterification reaction

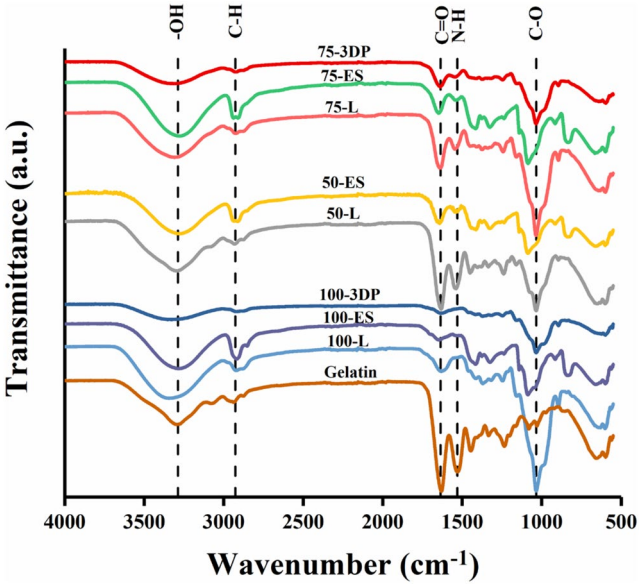

FIGURE 4 | FTIR spectrum of all the fabricated 3D scaffolds; 3DP: 3D printed scaffolds, ES: electrospun scaffolds, L: lyophilized scaffolds. [Color figure can be viewed at wileyonlinelibrary.com]

between —COOH and —OH groups [36]. The shift in the peak for C—O stretching in the electrospun scaffolds was attributed to the interactions between PH, G, and PVA. All the electrospun scaffolds showed additional peaks at around 837 cm^{-1} (deformation vibration of C—H bonds) and 1414 cm^{-1} (O—H bending of alcohol) which are characteristics for PVA [37, 38]. Thus, the FTIR spectrum shows the characteristic peaks for psyllium husk, gelatin, and PVA, thereby denoting their presence after scaffold fabrication.

4.3 | Swelling and Degradation Profile of the Fabricated 3D Scaffolds

The 3D scaffolds were studied for their swelling behavior over a period of 3 days. It can be observed (Figure 5a) that 100-3DP and 100-L have the maximum swelling percentage at the end of the day 3. The order of swelling percentage was observed as follows: 75-L > 100-ES > 50-L > 75-3DP > 50-ES > 75-ES. In all scaffold fabrication methods, the order of swelling was as follows: 100 > 75 > 50. This pattern of swelling behavior was observed based on the extent of crosslinking of the scaffolds by EDC-NHS. Based on the swelling data, the scaffolds consisting of equal amounts of PH and G (50-ES and 50-L) showed a greater extent of crosslinking than other scaffolds. In the scaffolds which consisted only of psyllium husk (100-3DP, 100-ES, and 100-L), the formation of amide bonds by EDC-NHS was not feasible, hence crosslinking occurred through ester linkages between —COOH and —OH groups [39, 40]. Swelling of scaffolds ensures the distribution of the culture medium and cells throughout the scaffolds; however, when the swelling degree is substantially greater, it would compromises the mechanical stability of the scaffolds. For this reason, an optimal level of crosslinking needs to be ensured while preparing the 3D scaffolds so that it does not affect swelling and mechanical stability of these scaffolds.

4.4 | Degradation of the 3D Scaffolds

From the electron microscopy images (Figure 5b) of the scaffolds immersed in PBS at 37°C for a period of 7 days, it was observed that the porous nature of the scaffolds fabricated through all the techniques (i.e., 3D printing, electrospinning, and lyophilization) was lost. In 3D printed scaffolds, two types of pores were observed—a macropore, because of 3D printing a specific geometry, and a micro/meso pore within the printed strand due to lyophilization. The 3D printed strands collapsed, leading to a reduced macropore size. In electrospun fibers, the scaffold lost its fiber-like structure in vitro. The fibers seemed to have fused together by day 7. In lyophilized scaffolds, an irregularity of the surface was observed. With an increase in psyllium husk polysaccharide content, the scaffold surface was observed to be achieving a sheet-like structure over the period of time.

4.5 | Morphological Examination and Functional Characterization of Hepatocytes Harvested From Rat Liver

In the present study, primary hepatocytes were harvested from rat liver by a double perfusion method using type IV collagenase enzyme (Figure 6). The harvesting method was optimized in order to achieve better cell density and also to obtain a homogeneous suspension of hepatocytes. In order to culture primary hepatocytes on the sterile culture dishes, they were coated with collagen (0.1 mg/mL). Cell culture studies were carried out with the initial concentration of 10^6 cells/scaffold. Hepatocytes were found to adhere well to the collagen-coated plastic substrates. They exhibited small aggregates after culturing for 24 h in the culture medium. Such small aggregates were found to be maintained in the culture, as shown, for up to 48 h (Figure 7); after which it was observed that hepatocytes were losing their membrane borders and forming small aggregates. In addition, hepatocytes exhibited the framework of actin filaments in the cortical region of the cells. Nuclei were found to be round or spherical in shape in all hepatocytes, revealing the harvesting and culture of healthy and viable cells. Furthermore, the functional characterization of hepatocytes was performed by the analysis of their metabolic performance such as glycogen storage, albumin, and urea secretion. By day 3, the albumin secreted by the primary hepatocytes was found to be in the range of ~0.09 mg/mL, which decreased to ~0.03 mg/mL by day 5. Urea was found to be ~26 μg/mL on day 3, which reduced to ~16 μg/mL by day 5. After staining the hepatocytes with periodic acid and Schiff's reagent, the cytoplasm was observed to be stained from purple to red, indicating the presence of glycogen storage in the isolated hepatocytes (Figure 7).

4.6 | Morphology of Primary Hepatocytes Cultured on Psyllium Polysaccharide-Based 3D Scaffolds

Primary hepatocytes were cultured successfully on all the psyllium polysaccharide-based 3D scaffolds (lyophilized, electrospun, and 3D printed) in several combinations. Their bright-field and electron microscopy images were captured to understand

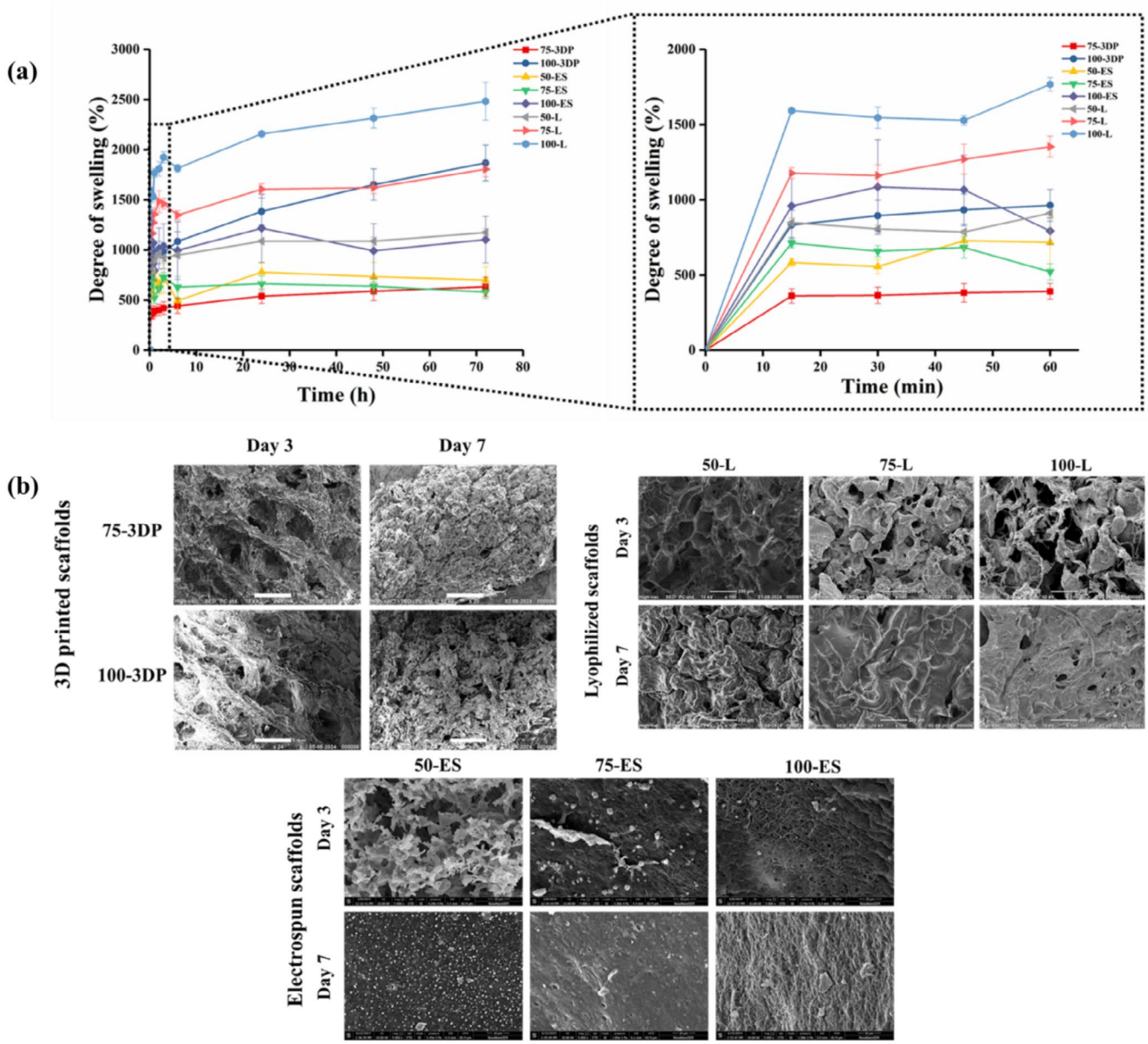

FIGURE 5 | (a) Graphical representation depicting the degree of swelling of the 3D scaffolds in PBS (pH 7.4) at 37°C and (b) scanning electron microscopy images showing degradation of 3D scaffolds in PBS (pH 7.4) at 37°C. [Color figure can be viewed at wileyonlinelibrary.com]

how hepatocytes are adhered to the scaffold's surface (Figure 8). Primary hepatocytes cultured on 3D scaffolds exhibited cuboidal morphology, dense aggregates, and restricted spreading compared to those on collagen-coated plastic substrates. After 24 h of incubation in the culture medium, hepatocytes cultured on 3D substrates formed multiple dense aggregates compared to fewer ones on collagen-coated plastic substrates. Aggregate formation on 3D scaffolds further enhanced significantly as the culture proceeded for 48 h. All the lyophilized, electrospun, and 3D printed scaffolds prepared with either psyllium polysaccharide alone or in combination with gelatin displayed a remarkable level of aggregate formation. The outcomes suggested that all the fabricated scaffolds significantly promoted the adhesion and aggregate formation of primary hepatocytes. Hepatocytes are known to exhibit optimal differentiated functions when they form 3D multicellular aggregates or spheroids compared to the monolayer 2D culture (Figures 7 and 8).

4.7 | Viability of Primary Hepatocytes Cultured on Psyllium Polysaccharide-Based 3D Scaffolds

The viability of primary hepatocytes after culturing them on the fabricated scaffolds was determined by MTT (3-[4,5-dimethyl-thiazol-2-yl]-2,5-diphenyltetrazolium bromide, HiMedia) reduction assay, which is based on the mitochondrial activity of the cell. The MTT (slightly yellow) is reduced to formazan crystals (purple) by mitochondrial dehydrogenases, indicating the cells are metabolically active. Absorbance was measured from solubilized formazan at 570 nm, and values were normalized to the control (collagen-coated 2D substrate) and set at 100%. The outcomes revealed (Figure 9) that all the fabricated psyllium polysaccharide-based 3D scaffolds significantly promoted the viability of primary hepatocytes compared to the control, with the 50-ES nanofibrous scaffold showing a maximum viability of 280%. These results indicated the potential of psyllium

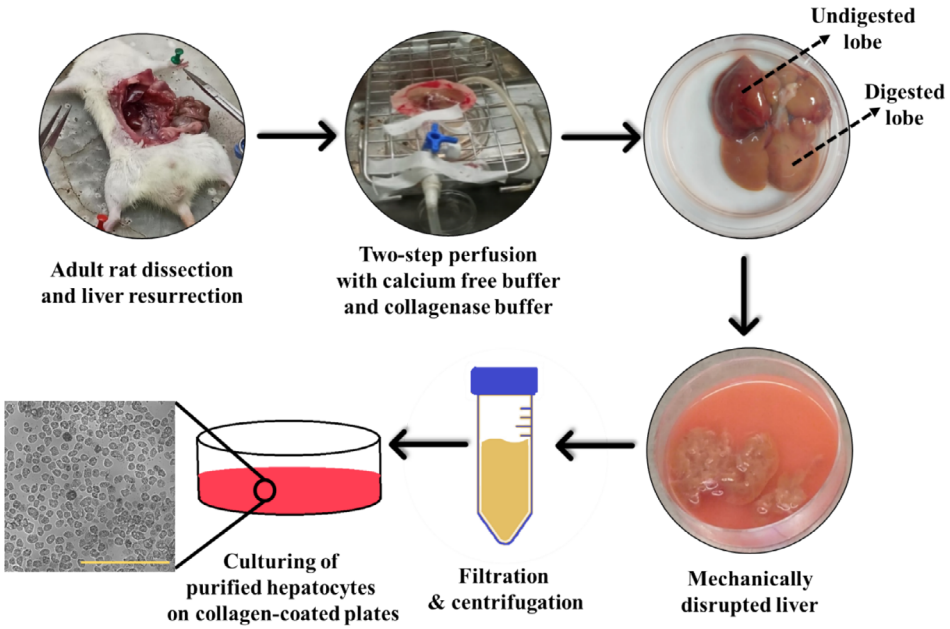

FIGURE 6 | Protocol for isolating and culturing hepatocytes from adult rats. [Color figure can be viewed at wileyonlinelibrary.com]

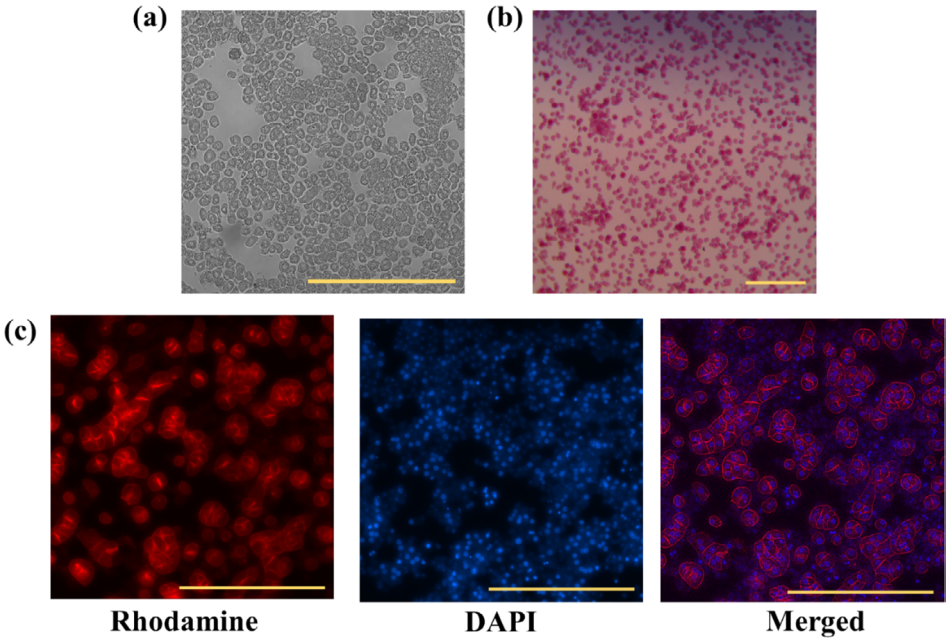

FIGURE 7 | (a) Bright-field images depicting the hepatocytes cultured after isolation from rat liver, (b) glycogen staining, and (c) primary hepatocytes after fluorescent staining. Scale bar: 200 μm. [Color figure can be viewed at wileyonlinelibrary.com]

polysaccharide for the culture and maintenance of the viability of primary hepatocytes in vitro.

4.8 | Functional Assessment of Primary Hepatocytes Cultured on Psyllium Polysaccharide-Based 3D Scaffolds by Measuring Albumin and Urea Secretion

Hepatocytes are the primary cell type present in the adult liver and perform several important functions, including secretion of plasma proteins, urea synthesis, and detoxification. Although there is no standardized value or acceptable concentration for showing the optimal cellular function, most of the reported studies suggest the measurement of albumin and urea as a biomarker for characterizing functionally efficient hepatocytes. Therefore, we have collected the culture medium after culturing hepatocytes on all the 3D scaffolds to measure the amount of albumin and urea secreted by the cells (Figures 10 and 11). The outcomes revealed that all the 3D scaffolds in either form supported hepatocytes to produce and secrete albumin and urea into the extracellular fluid, indicating the performance of hepatocytes functionally similar to the in vivo condition. In general, the albumin and urea secretion were found to be comparatively lower in 100% psyllium polysaccharide scaffolds; moreover, they were found to be decreasing

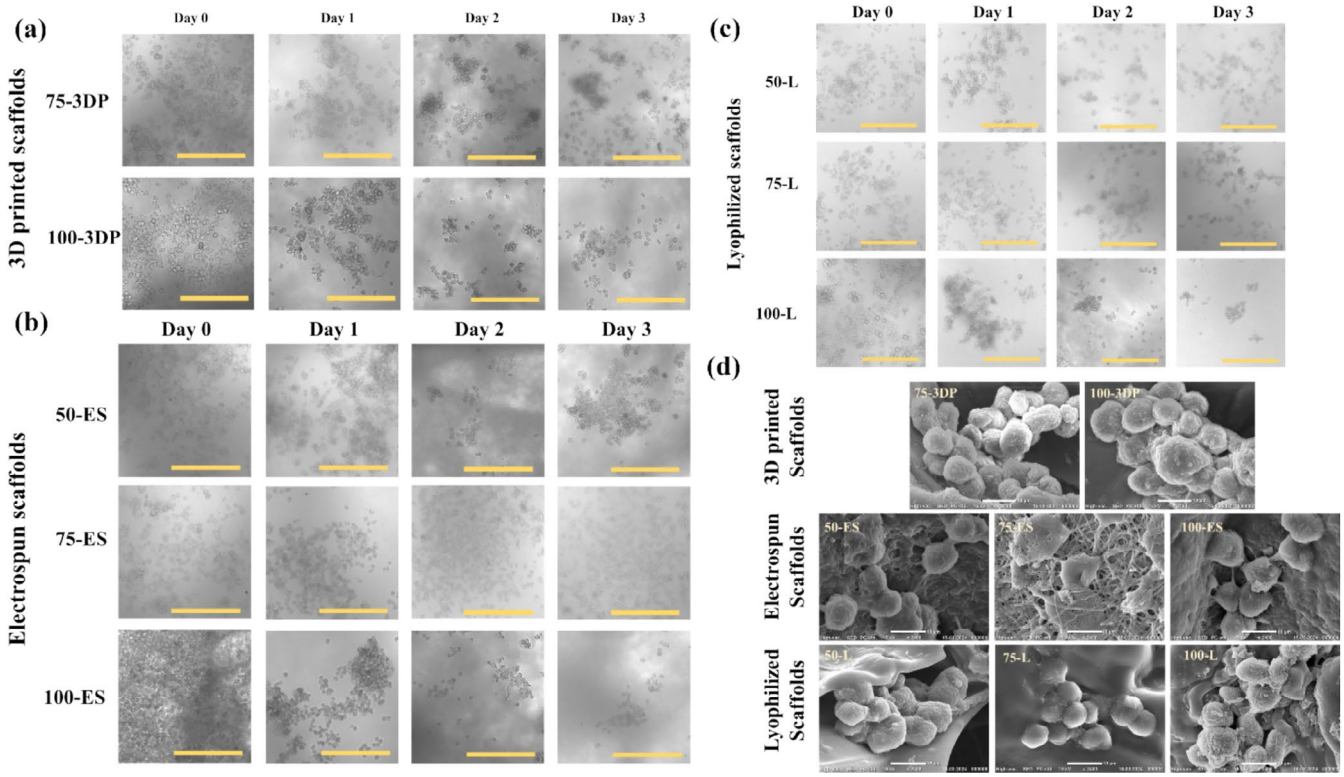

FIGURE 8 | Bright-field microscopic images of hepatocytes cultured on (a) 3D printed, (b) electrospun and (c) lyophilized scaffolds (Scale bar: 200 μm). (d) Scanning electron microscopic images of hepatocytes cultured on all the fabricated 3D scaffolds (Scale bar: 10 μm). [Color figure can be viewed at wileyonlinelibrary.com]

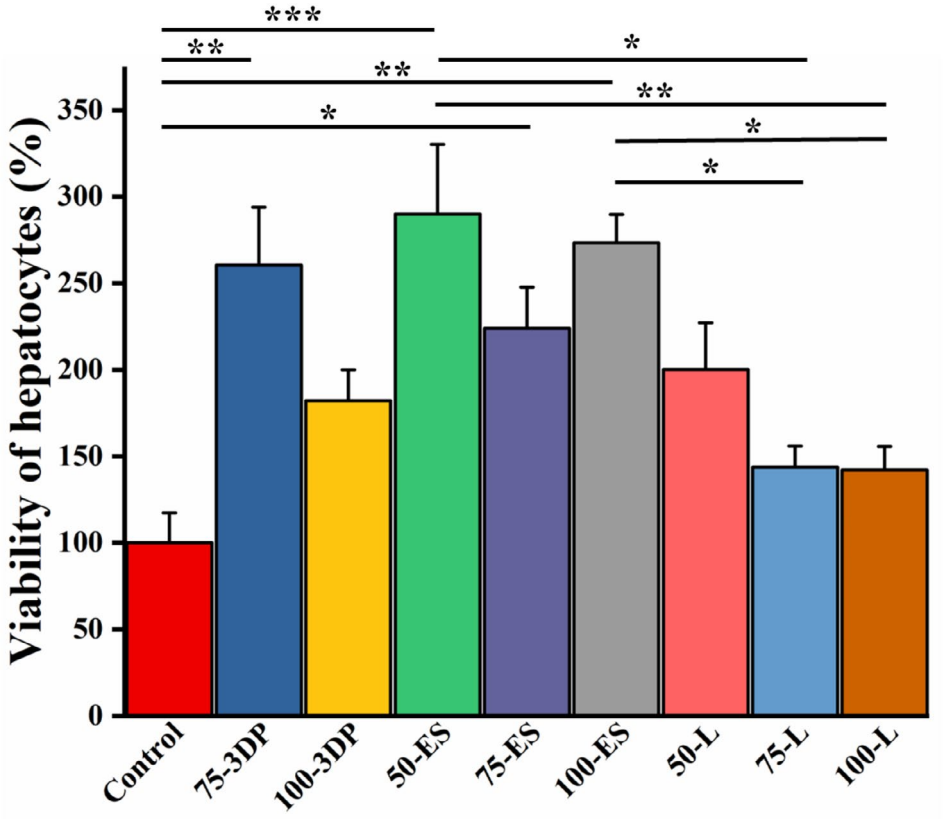

FIGURE 9 | Percentage of cell viability of hepatocytes seeded on collagen-coated 2D plastic substrate and 3D psyllium polysaccharide-based scaffolds; 3DP: 3D printed scaffolds, ES: electrospun scaffolds, L: lyophilized scaffolds. [Color figure can be viewed at wileyonlinelibrary.com]

from day 3 to day 5. The 100% psyllium polysaccharide scaffolds were crosslinked possibly through ester bonds with the help of EDC-NHS crosslinker. Since the ester bond is prone to hydrolysis, such scaffolds are likely to undergo degradation at a faster pace compared to the other scaffold combinations, resulting in cell detachment from their surface.

5 | Discussion

The essence of tissue engineering lies in replicating the body's architectural intricacies and proper cell–cell interactions. Several scaffold materials, from natural to synthetic, are being explored to mimic the native tissue-like extracellular microenvironment. Among these, polymers have significant relevance due to their chemical tunability, enabling the materials to have appropriate mechanical, physical, and biological properties. With the advancement in tissue engineering, the use of plant-derived biopolymers such as alginate, guar gum, *Aloe vera* gel, to name a few, has gained a noted momentum. *Plantago ovata* or psyllium husk (isabgol) is one of the most widely used biocompatible, biodegradable, and commercially available plant-derived polysaccharides in biomedical, pharmaceutical, and food industries. Recently, psyllium polysaccharide hydrogel has shown tremendous potential for tissue engineering and drug delivery applications. Functionally modified psyllium with polyacrylic acid (PAA) has been used as a superabsorbent hydrogel to prove its potential in drug delivery applications [41].

In general, hepatocytes are found to form spheroids and get trapped between the pores in the 3D scaffold. Due to this, the cells are not properly anchored on the scaffold surface, leading to a hindrance of their functional efficiency. We have investigated

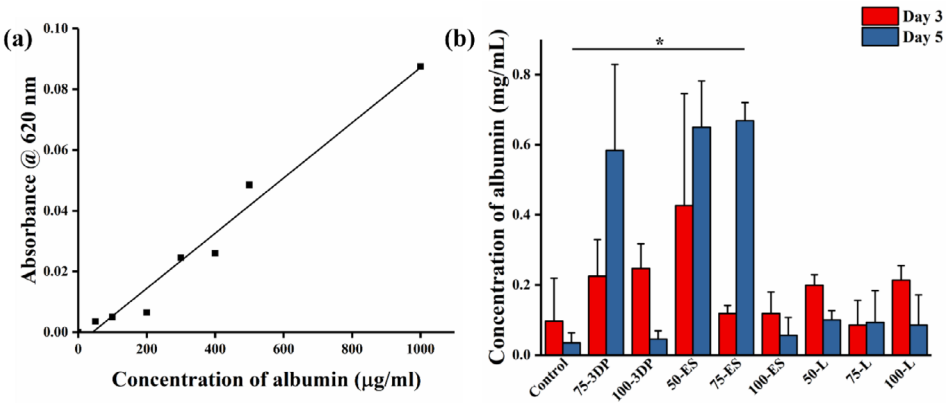

FIGURE 10 | Graphical representation of (a) standard curve of albumin ($R^2 = 0.97211$) and (b) amount of albumin (mg/mL) secreted by hepatocytes when cultured on collagen-coated 2D plastic substrate and psyllium polysaccharide-based 3D scaffolds; 3DP: 3D printed scaffolds, ES: electrospun scaffolds, L: lyophilized scaffolds. [Color figure can be viewed at wileyonlinelibrary.com]

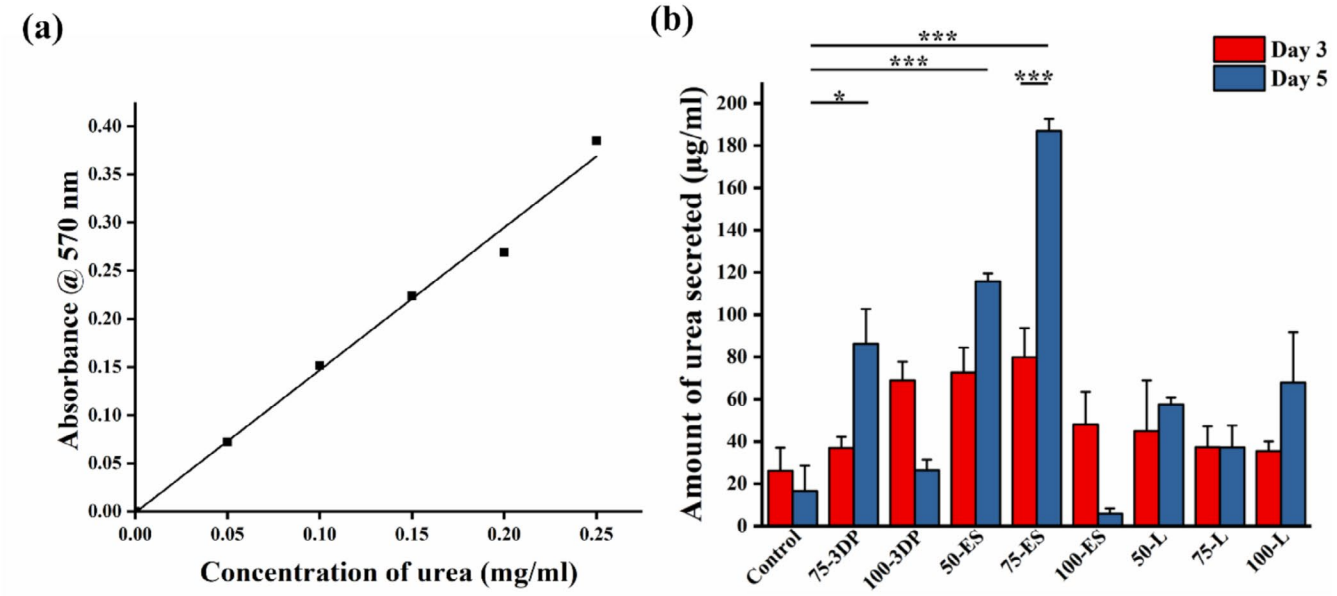

FIGURE 11 | Graphical representation of (a) standard curve of urea ($R^2 = 0.98993$) and (b) amount of urea (µg/mL) secreted by hepatocytes when cultured on collagen-coated plastic 2D substrate and psyllium polysaccharide-based 3D scaffolds; 3DP: 3D printed scaffolds, ES: electrospun scaffolds, L: lyophilized scaffolds. [Color figure can be viewed at wileyonlinelibrary.com]

the potential of psyllium polysaccharide-based hydrogel in various forms, including lyophilized, electrospun, and 3D printed scaffolds for hepatocyte culture and their functional performance. The scaffold fabrication process was optimized to obtain a stable end product. The solute concentration of the polysaccharide and the protein was selected based on their printability (for 3D printing) and spinnability (for electrospinning). EDC-NHS is a chemical crosslinker that aids in the formation of amide and ester bonds. The solvent for the crosslinkers was chosen according to the experimental need. Psyllium husk has the capacity to absorb water and swell [42] to a great extent, depending on the polysaccharide concentration. When water was used as a solvent for crosslinkers for the 3D printed scaffolds, it was observed that the rate of crosslinking was less than the water absorption and swelling, leading to the disintegration of the printed constructs. Therefore, ethanol was chosen as the suitable solvent for this work. As a standard protocol, all the scaffolds were crosslinked with EDC-NHS mixed in an ethanol solvent.

The morphological information was obtained from the SEM images of the scaffolds. An effort was made to reduce the space between 3D printed strands up to the minimum possible distance while designing the computer-aided design file for 3D printing the hydrogel. In addition, after the height interval of 0.2 mm, each layer was rotated at an angle of 50° parallel to the previous layer during the printing of the scaffold, giving rise to a complex network of 3D printed strands with the porous space significantly reduced up to the range of 200–240 μm (macropores) when the printed 3D scaffolds were placed in an aqueous environment. Apart from macropores, which help in media, gas exchange, and even-cell distribution, some micro/meso pores appeared on the surface of the printed strands when lyophilized post-printing. These aid in anchoring the hepatocytes seeded on the scaffold. Similarly, a network of randomly oriented nanofibers in multiple layers was observed in the case of electrospun sheets, where its porosity enhanced the diffusion of growth factors and medium. These fibers are said to promote cellular activity by resembling a native tissue's ECM [43]. Here, we observed that the fiber diameter of the electrospun sheets increased with an increase in psyllium husk content (50-ES > 75-ES > 100-ES). This phenomenon was observed because of the viscosity of the spinning solution. When the psyllium husk content increases, the viscosity of the solution also increases. An increase in viscosity leads to a higher viscoelastic force and resists the stretching of the polymeric solution during the spinning process. This would yield fibers with larger diameters [44]. Reported studies have suggested a pore size of 50–200 μm suitable for culture and maintenance of hepatocytes [45] and of 160–270 μm in promoting angiogenesis [46]. Our results show that all the scaffolds, when placed in the aqueous medium, exhibit porous space in the similar size range, which supports their suitability for hepatocyte culture.

The ATR-FTIR spectrum of the crosslinked scaffolds reveals the presence of peaks that belong to psyllium husk and gelatin. The presence of the amide bond is known from the peaks contributing to C═O, N—H bending, and C—N stretching [34]. The peaks for the ester bond are known from the C—O stretching peak. The crosslinking efficiency of the scaffold was also observed from the swelling data. The scaffolds at physiological pH and temperature exhibited swelling behavior according to the fabrication methods. The electrospun scaffolds showed the least swelling behavior compared to lyophilized and 3D printed scaffolds. The swelling of the scaffolds also seems to depend on the concentration of psyllium polysaccharide used. In any case, of the fabricated scaffold, the swelling behavior increases with increased psyllium husk content. The scaffolds with an equal proportion of psyllium husk and gelatin (50-ES and 50-L) exhibited the least swelling. As explained before, the crosslinking of the scaffolds significantly impacts the swelling behavior. Since the 50-ES and 50-L scaffolds are likely to contain more amide bond formation compared to the rest of the scaffold combinations, the swelling behavior was found to be limited in such scaffolds. Amide bonds are said to be more stable than ester bonds. In pure psyllium husk scaffolds, the crosslinking had occurred likely through ester bond formation, a possible reason why they are prone to hydrolysis and are less stable comparatively. The degradation of the scaffolds was observed from the topographical information obtained through SEM images. From observation, the scaffolds were undergoing degradation at physiological pH and temperature, along with a reduction of pore size, over a 7-day period.

The primary hepatocytes from adult rats were successfully harvested and cultured on collagen-coated standard substrates using the double perfusion method. Morphological observation through the microscopic images and functional assessment through the measurement of albumin and urea secretion revealed the successful collection of mature hepatocytes from the rat liver. Hepatocytes exhibited the framework of actin filaments in the cortical region of the cells. In addition, nuclei were found spherical in all hepatocytes, revealing the harvesting and culture of healthy and viable cells. Usually, primary hepatocytes exhibit an extended and flattened shape when cultured on a 2D substrate [47]. Similarly, it can be observed from the bright-field and fluorescent images that the isolated hepatocytes adapted a flattened structure with well-developed cell–cell adhesion. Instead of a spheroid formation, the hepatocytes cultured on 2D collagen-coated substrates formed close associations. Moreover, the hepatocytes cultured on 2D substrate exhibited optimal levels of albumin and urea secretion. However, when the same hepatocytes were cultured on the 3D scaffolds fabricated by various techniques, they displayed aggregate formation, as evident from the bright-field and electron microscopy images. From the SEM images, we can clearly observe the cells tightly bound with each other, forming aggregates, and the entire aggregate anchoring to the surface of the scaffold. All scaffold combinations, either psyllium polysaccharide alone or with gelatin, evinced this phenomenon. These results suggested that all the fabricated scaffolds significantly promoted primary hepatocyte adhesion and aggregate formation. Such observation is hypothesized to be the result of interactions between asialoglycoprotein receptors (ASGPR) on the hepatocyte surface and galactose (on psyllium husk), thereby anchoring the cells, and enhancing their spheroid formation. The role of ASGPR receptors binding to galactose moieties and enhancing the activity of the hepatocytes was already evident [48].

In coherence with the morphological observations, viability assays showed that all the fabricated psyllium polysaccharide-based 3D scaffolds significantly enhanced the viability of primary hepatocytes compared to collagen-coated 2D plastic

substrates. However, electrospun nanofibrous sheets fabricated using either psyllium polysaccharide alone or in combination with gelatin maintained a slightly higher viability of the cells in comparison to lyophilized and 3D printed scaffolds. Thus, the outcomes revealed that psyllium polysaccharide could be useful for the culture and maintenance of the viability of primary hepatocytes in vitro. In addition, the measurement of albumin and urea secretion indicated that the performance of hepatocytes in vitro was functionally similar to that of the in vivo condition. Results showed that all the scaffold combinations enhanced the functioning of hepatocytes compared to the collagen-coated 2D substrates. Although all the hepatocytes cultured on scaffolds showed enhanced albumin and urea production compared to the hepatocytes cultured on collagen-coated plates, the statistical significance of the obtained data, as found using the one-way ANOVA Tukey post hoc test, suggested that 75-3DP, 75-ES, and 50-ES scaffolds delivered significantly an increased amount of viability and functioning of the hepatocytes cultured in vitro (Table 2). The key physicochemical aspect of the 3D printed scaffolds (75-3DP) and the electrospun scaffolds (50-ES, 75-ES) demonstrating superior hepatocyte functionality compared to other scaffolds is possibly their architecture and swelling behavior. Their interconnected porous structure and filamentous arrangement mimic the extracellular matrix (ECM) in vitro. The lyophilized scaffolds could not achieve this ECM-like structure. In addition, lyophilized scaffolds also exhibited the highest swelling degree compared to the other scaffolds. It is postulated that the filamentous arrangement with controlled pore size in the 3D printed scaffolds and the fibrous architecture of electrospun scaffolds might favor their limited swelling behavior, thereby limiting the loss of adhered cells. Also, when observed, the pure psyllium polysaccharide scaffolds (100-3DP and 100-ES) exhibited higher swelling behavior than 75-3DP, 50-ES, and 75-ES scaffolds. This could be attributed to the amide bond formation between the carboxylic and amine groups in the case of 75-3DP, 50-ES, and 75-ES scaffolds and the ester bond formation between the carboxylic and hydroxyl groups in the case of 100-3DP and 100-ES scaffolds when the fabricated scaffolds were

TABLE 2 | One-way ANOVA with Tukey's post hoc means of comparison performed between the groups. Results are considered statistically significant when $p < 0.05$ (*), $p < 0.01$ (**), $p < 0.001$ (***); no significance is indicated by '-'; 3DP: 3D printed scaffolds, ES: electrospun scaffolds, L: lyophilized scaffolds.

Scaffolds	Assays	Control	75-3DP	100-3DP	50-ES	75-ES	100-ES	50-L	75-L	100-L
75-3DP	Viability (48 h)	**	—	—	—	—	—	—	—	—
	Albumin (Day 5)	—	—	—	—	—	**	—	—	—
	Urea (Day 5)	*	—	—	—	***	**	—	—	—
100-3DP	Viability (48 h)	—	—	—	—	___	—	—	—	—
	Albumin (Day 5)	—	—	—	—	*	—	—	—	—
	Urea (Day 5)	—	—	—	***	***	—	—	—	—
50-ES	Viability (48 h)	***	—	—	—	—	—	—	*	**
	Albumin (Day 5)	—	—	—	—	—	—	—	—	—
	Urea (Day 5)	***	—	***	—	*	***	—	**	—
75-ES	Viability (48 h)	*	—	—	—	—	—	—	—	—
	Albumin (Day 5)	*	—	*	—	—	—	—	—	—
	Urea (Day 5)	***	***	***	*	—	***	***	***	***
100-ES	Viability (48 h)	**	—	—	—	—	—	—	*	*
	Albumin (Day 5)	—	—	—	—	—	—	—	—	—
	Urea (Day 5)	—	**	—	***	***	—	—	—	—
50-L	Viability (48 h)	—	—	—	—	—	—	—	—	—
	Albumin (Day 5)	—	—	—	—	—	—	—	—	—
	Urea (Day 5)	—	—	—	—	***	—	—	—	—
75-L	Viability (48 h)	—	—	—	*	—	*	—	—	—
	Albumin (Day 5)	—	—	—	—	—	—	—	—	—
	Urea (Day 5)	—	—	—	**	***	—	—	—	—
100-L	Viability (48 h)	—	—	—	**	—	*	—	—	—
	Albumin (Day 5)	—	—	—	—	—	—	—	—	—
	Urea (Day 5)	—	—	—	—	***	—	—	—	—

subjected to EDC-NHS crosslinking. The ester bonds are not as stable as the amide bonds. Hence, the higher level of swelling behavior was observed in 100-3DP and 100-ES scaffolds. The psyllium husk polysaccharide-based scaffolds developed in this study utilize low-cost raw materials that are easy to mold into a functional scaffold without tedious prerequisite processing. The psyllium husk and gelatin were utilized in their commercial forms without any further chemical or physical modification of the raw materials. Generally, most of the liver tissue scaffolds are made of collagen [14] or decellularized liver matrix. Although the functioning of hepatocytes is said to be significantly enhanced on such scaffolds, the fabrication technology involves tedious processing and is expensive. The flexibility of the materials to be used in a straight-cut fabrication technology such as electrospinning and 3D printing, and furthermore the display of their enhanced hepatocyte functioning, makes them more favorable for their application in liver tissue engineering. Thus, the outcomes suggest that psyllium polysaccharide in 3D scaffolds could be potentially helpful for the culture and maintenance of primary hepatocytes in vitro.

6 | Conclusion

In the present study, the potential of psyllium husk polysaccharide hydrogel either alone or in combination with gelatin has been explored for the culture and maintenance of primary adult rat hepatocytes. Various forms of scaffolds, including lyophilized porous templates, electrospun nanofibrous sheets, and 3D printed complex structures using psyllium polysaccharide were designed and fabricated. Primary hepatocytes harvested from the rat liver by the double perfusion method using collagenase were cultured on all the fabricated 3D scaffolds. The scaffolds placed in the aqueous medium exhibited porous space in a size range of 100–250 μm, supporting their suitability for hepatocyte culture. In addition, the 3D printed scaffolds exhibited both micro and macro pores in the same scaffold that helped in anchoring and distributing hepatocytes throughout the scaffold. To the best of our knowledge, the fabrication of such a scaffold comprising both micro and macro pores is reported for the first time. The combination of 3D printing (for creating macropores) and lyophilization (for creating micro/mesopores) techniques was deemed best to create such scaffolds. All the 3D scaffolds prepared with either psyllium polysaccharide alone or in combination with gelatin displayed significantly enhanced viability of primary hepatocytes and a remarkable level of aggregate formation compared to those on collagen-coated 2D plastic substrates. Their functional analysis of albumin and urea secretion was also significantly higher than those of the collagen-coated 2D substrates. Moreover, 75-3DP, 50-ES, and 75-ES scaffolds exhibited statistically significant enhanced functioning and viability of hepatocytes. The viability of hepatocytes cultured on these scaffolds was found to be 210%–270% compared to the collagen-coated 2D plastic substrates. The albumin (up to 0.6 mg/mL) and urea (up to 180 μg/mL) secretion were also found noticeably enhanced when observed over a period of 5 days. Thus, we anticipate that, given the presence of a significant amount of galactose residues in their polymeric network, the psyllium polysaccharide-based hydrogel has significant potential for the culture and maintenance of primary hepatocytes in vitro.

Author Contributions

Sushmitha Paulraj: data curation (lead), formal analysis (lead), investigation (lead), methodology (lead), visualization (lead), writing – original draft (lead), writing – review and editing (lead). **Dhanvi Vedantham:** data curation (supporting), investigation (supporting), methodology (supporting), writing – original draft (supporting). **Pooja Kumari:** data curation (supporting), investigation (supporting), writing – review and editing (supporting). **Priya Singh:** methodology (supporting), writing – review and editing (supporting). **Snehlata Yadav:** writing – review and editing (supporting). **Sanjeev Kumar Mahto:** conceptualization (lead), funding acquisition (lead), project administration (lead), resources (lead), supervision (lead), validation (equal), writing – review and editing (equal).

Acknowledgments

The authors would like to thank the Core Research Grant (CRG) from the Science and Engineering Research Board (SERB), Department of Science and Technology, Government of India (CRG/2020/000235) for financially supporting this work.

Ethics Statement

The animals used in this study were approved by the Institute Animal Ethical Committee, Indian Institute of Technology (Banaras Hindu University). Approval No: IIT(BHU)/IAEC/2022/067 and IIT(BHU)/IAEC/2023/061.

Conflicts of Interest

The authors declare no conflicts of interest.

Data Availability Statement

The authors confirm that the data supporting the findings of this study are available within the article.

References

1. S. K. Asrani, H. Devarbhavi, J. Eaton, and P. S. Kamath, "Burden of Liver Diseases in the World," *Journal of Hepatology* 70 (2019): 151–171.

2. J. Zhang, H. F. Chan, H. Wang, D. Shao, Y. Tao, and M. Li, "Stem Cell Therapy and Tissue Engineering Strategies Using Cell Aggregates and Decellularized Scaffolds for the Rescue of Liver Failure," *Journal of Tissue Engineering* 12, no. 2 (2021): 041731420986711.

3. K. Nagaraja, P. Dhokare, A. Bhattacharyya, and I. Noh, "Recent Advances in 3D Bioprinting of Polysaccharide-Based Bioinks for Fabrication of Bioengineered Tissues," *Molecular Systems Design & Engineering* 9, no. 10 (2024): 977–999, https://doi.org/10.1039/d4me00001c.

4. S. Sasikumar, A. Boden, S. Chameettachal, et al., "Galactose Tethered Decellularized Liver Matrix: Toward a Biomimetic and Biofunctional Matrix for Liver Tissue Engineering," *ACS Applied Bio Materials* 5, no. 6 (2022): 3023–3037.

5. S. Kammerer, "Three-Dimensional Liver Culture Systems to Maintain Primary Hepatic Properties for Toxicological Analysis In Vitro," *International Journal of Molecular Sciences* 22, no. 10 (2021): 214.

6. S. Alonso, "Exploiting the Bioengineering Versatility of Lactobionic Acid in Targeted Nanosystems and Biomaterials," *Journal of Controlled Release* 287 (2018): 216–234.

7. R. S. Stowers, "Advances in Extracellular Matrix-Mimetic Hydrogels to Guide Stem Cell Fate," *Cells, Tissues, Organs* 211 (2022): 703.

8. J. Christoffersson, C. Aronsson, M. Jury, R. Selegård, D. Aili, and C.-F. Mandenius, "Fabrication of Modular Hyaluronan-PEG Hydrogels

to Support 3D Cultures of Hepatocytes in a Perfused Liver-On-a-Chip Device," *Biofabrication* 11, no. 1 (2018): 015013, https://doi.org/10.1088/1758-5090/aaf657.

9. X.-F. Tong, F.-Q. Zhao, Y.-Z. Ren, Y. Zhang, Y.-L. Cui, and Q.-S. Wang, "Injectable Hydrogels Based on Glycyrrhizin, Alginate, and Calcium for Three-Dimensional Cell Culture in Liver Tissue Engineering," *Journal of Biomedical Materials Research. Part A* 106 (2018): 3292–3302.

10. Z. Su, P. Li, B. Wu, et al., "PHBVHHx Scaffolds Loaded With Umbilical Cord-Derived Mesenchymal Stem Cells or Hepatocyte-Like Cells Differentiated From These Cells for Liver Tissue Engineering," *Materials Science & Engineering. C, Materials for Biological Applications* 45 (2014): 374–382.

11. A. Tripathi and J. S. Melo, "Preparation of a Sponge-Like Biocomposite Agarose–Chitosan Scaffold With Primary Hepatocytes for Establishing an In Vitro 3D Liver Tissue Model," *RSC Advances* 5 (2015): 30701–30710.

12. Y. Wu, Z. Y. W. Lin, A. C. Wenger, K. C. Tam, and X. S. Tang, "3D Bioprinting of Liver-Mimetic Construct With Alginate/Cellulose Nanocrystal Hybrid Bioink," *Bioprinting* 9 (2018): 1.

13. R. Senthil, "Silk Fibroin Sponge Impregnated With Fish Bone Collagen: A Promising Wound Healing Scaffold and Skin Tissue Regeneration," *International Journal of Artificial Organs* 47 (2024): 338–346.

14. Y. Zhao, Y. Xu, B. Zhang, et al., "In VivoGeneration of Thick, Vascularized Hepatic Tissue From Collagen Hydrogel-Based Hepatic Units," *Tissue Engineering Part C: Methods* 16 (2010): 653–659.

15. S. Ye, J. W. B. Boeter, L. C. Penning, B. Spee, and K. Schneeberger, "Hydrogels for Liver Tissue Engineering," *Bioengineering (Basel)* 6 (2019): 59.

16. M. W. Davis and J. P. Vacanti, "Toward Development of an Implantable Tissue Engineered Liver," *Biomaterials* 17 (1996): 365–372.

17. S. S. Ng, A. Xiong, K. Nguyen, et al., "Long-Term Culture of Human Liver Tissue With Advanced Hepatic Functions," *JCI Insight* 2, no. 11 (2017): e90853, https://doi.org/10.1172/jci.insight.90853.

18. R. Hammink, L. J. Eggermont, T. Zisis, et al., "Affinity-Based Purification of Polyisocyanopeptide Bioconjugates," *Bioconjugate Chemistry* 28 (2017): 2560–2568.

19. J. Kasuya, R. Sudo, R. Tamogami, et al., "Reconstruction of 3D Stacked Hepatocyte Tissues Using Degradable, Microporous Poly(-Lactide-Co-Glycolide) Membranes," *Biomaterials* 33 (2012): 2693–2700.

20. R. Senthil, W. S. Vedakumari, S. Basavarajappa, et al., "Gelatin/Nanofibrin Bioactive Scaffold Prepared With Enhanced Biocompatibility for Skin Tissue Regeneration," *Journal of Saudi Chemical Society* 27 (2023): 101–747.

21. S. Rethinam, "Preparation of Bioscaffold Supported by Chitosan and Nanocurcumin to Promote Tissue Engineering," *Regenerative Engineering and Translational Medicine* 10 (2024): 553–563.

22. R. Senthil, S. B. Kavukcu, and W. S. Vedakumari, "Cellulose Based Biopolymer Nanoscaffold: A Possible Biomedical Applications," *International Journal of Biological Macromolecules* 246 (2023): 125–656.

23. W. Zhao, S. Cao, H. Cai, et al., "Chitosan/Silk Fibroin Biomimic Scaffolds Reinforced by Cellulose Acetate Nanofibers for Smooth Muscle Tissue Engineering," *Carbohydrate Polymers* 298 (2022): 120056, https://doi.org/10.1016/j.carbpol.2022.120056.

24. B. Wang, Q. Hu, T. Wan, et al., "Porous Lactose-Modified Chitosan Scaffold for Liver Tissue Engineering: Influence of Galactose Moieties on Cell Attachment and Mechanical Stability," *International Journal of Polymeric Science* 2016, no. 2 (2016): 738–862.

25. F. Ghahremanzadeh, F. Alihosseini, and D. Semnani, "Investigation and Comparison of New Galactosylation Methods on PCL/Chitosan Scaffolds for Enhanced Liver Tissue Engineering," *International Journal of Biological Macromolecules* 174 (2021): 278–288.

26. E. S. Mirdamadi, Z. Khosrowpour, D. Jafari, M. Gholipourmalekabadi, and M. Solati-Hashjin, "3D-Printed PLA/Gel Hybrid in Liver Tissue Engineering: Effects of Architecture on Biological Functions," *Biotechnology and Bioengineering* 120 (2023): 836–851.

27. P. L. Lewis, R. M. Green, and R. N. Shah, "3D-Printed Gelatin Scaffolds of Differing Pore Geometry Modulate Hepatocyte Function and Gene Expression," *Acta Biomaterialia* 69 (2018): 63–70.

28. Y. Zhang, L. Li, L. Dong, et al., "Hydrogel-Based Strategies for Liver Tissue Engineering," *Chem & Bio Engineering* 1 (2024): 887–915.

29. X. Sui, H. Zhang, J. Yao, et al., "3D Printing of 'Green' Thermo-Sensitive Chitosan-Hydroxyapatite Bone Scaffold Based on Lyophilized Platelet-Rich Fibrin," *Biomedical Materials* 18, no. 2 (2023): 025022, https://doi.org/10.1088/1748-605X/acbad5.

30. Y. Dan, O. Liu, Y. Liu, et al., "Development of Novel Biocomposite Scaffold of Chitosan-Gelatin/Nanohydroxyapatite for Potential Bone Tissue Engineering Applications," *Nanoscale Research Letters* 11 (2016): 487.

31. X. Liu, X. Yao, Q. OuYang, A. L. Oliveira, L. Yan, and Y. Zhang, "Nanofiber Scaffold-Based Tissue Engineering for the Treatment of Acute Liver Failure," *Advanced Fiber Materials* 6 (2024): 686–712.

32. L. E. Bertassoni, "Bioprinting of Complex Multicellular Organs With Advanced Functionality—Recent Progress and Challenges Ahead," *Advanced Materials* 34, no. 2 (2022): 101.

33. S. Poddar, P. S. Agarwal, A. K. Sahi, et al., "Fabrication and Cytocompatibility Evaluation of Psyllium Husk (Isabgol)/Gelatin Composite Scaffolds," *Applied Biochemistry and Biotechnology* 188 (2019): 750–768.

34. Ö. Yildirim-Semerci, R. Bilginer-Kartal, and A. Arslan-Yildiz, "Arabinoxylan-Based Psyllium Seed Hydrocolloid: Single-Step Aqueous Extraction and Use in Tissue Engineering," *International Journal of Biological Macromolecules* (2024): 131856.

35. I. C. Ng, L. Zhang, N. N. Y. Y. Shen, et al., "Isolation of Primary Rat Hepatocytes with Multiparameter Perfusion Control," *Journal of Visualized Experiments* (2021): 170.

36. S. Poddar, P. S. Agarwal, A. K. Sahi, N. Varshney, K. Y. Vajanthri, and S. K. Mahto, "Fabrication and Characterization of Electrospun Psyllium Husk-Based Nanofibers for Tissue Regeneration," *Journal of Applied Polymer Science* 138, no. 24 (2021): 50569, https://doi.org/10.1002/app.50569.

37. H. Abral, A. Atmajaya, M. Mahardika, et al., "Effect of Ultrasonication Duration of Polyvinyl Alcohol (PVA) Gel on Characterizations of PVA Film," *Journal of Materials Research and Technology* 9 (2020): 2477–2486.

38. I. Jipa, A. Stoica, M. Stroescu, et al., "Potassium Sorbate Release From Poly(Vinyl Alcohol)-Bacterial Cellulose Films," *Chemical Papers* 66 (2012): 66.

39. R. S. Gonçalves, A. C. V. De Oliveira, N. Hioka, and W. Caetano, "Synthesis and Characterization of 5(6)-Carboxyfluorescein-Conjugated F127 and 10R5 Copolymers as Potential Water-Soluble Fluorescence Probes," *Chemical Data Collections* 30 (2020): 100557.

40. P. F. Gratzer and J. M. Lee, "Control of pH Alters the Type of Cross-Linking Produced by 1-Ethyl-3-(3-Dimethylaminopropyl)-Carbodiimide (EDC) Treatment of Acellular Matrix Vascular Grafts," *Journal of Biomedical Materials Research* 58 (2001): 172–179.

41. S. M. Hosseini, M. Shahrousvand, S. Shojaei, H. A. Khonakdar, A. Asefnejad, and V. Goodarzi, "Preparation of Superabsorbent Eco-Friendly Semi-Interpenetrating Network Based on Cross-Linked Poly Acrylic Acid/Xanthan Gum/Graphene Oxide (PAA/XG/GO): Characterization and Dye Removal Ability," *International Journal of Biological Macromolecules* 152 (2020): 884–893.

42. R. Agrawal, *Dietary Fibers* (IntechOpen, 2021).

43. J. A. Smith and E. Mele, "Electrospinning and Additive Manufacturing: Adding Three-Dimensionality to Electrospun Scaffolds for Tissue Engineering," *Frontiers in Bioengineering and Biotechnology* 9 (2021): 674738, https://doi.org/10.3389/fbioe.2021.674738.

44. R. M. Nezarati, M. B. Eifert, and E. Cosgriff-Hernandez, "Effects of Humidity and Solution Viscosity on Electrospun Fiber Morphology," *Tissue Engineering. Part C, Methods* 19 (2013): 810–819.

45. J. Rodriguez-Fernandez, E. Garcia-Legler, E. Villanueva-Badenas, et al., "Primary Human Hepatocytes-Laden Scaffolds for the Treatment of Acute Liver Failure," *Biomaterials Advances* 153 (2023): 213–576.

46. A. Zaeri, K. Cao, F. Zhang, R. Zgeib, and R. C. Chang, "A Review of the Structural and Physical Properties That Govern Cell Interactions With Structured Biomaterials Enabled by Additive Manufacturing," *Bioprinting* 26 (2022): e00201.

47. Y. C. Wu, G. X. Wu, K. W. Chen, et al., "Transplantation of 3D Adipose-Derived Stem Cell/Hepatocyte Spheroids Alleviates Chronic Hepatic Damage in a Rat Model of Thioacetamide-Induced Liver Cirrhosis," *Scientific Reports* 12 (2022): 1227.

48. K. S. Vasanthan, S. Sethuraman, and M. Parthasarathy, "Electrochemical Evidence for Asialoglycoprotein Receptor – Mediated Hepatocyte Adhesion and Proliferation in Three Dimensional Tissue Engineering Scaffolds," *Analytica Chimica Acta* 890 (2015): 83–90.